Analysing the Lake Urmia restoration progress using ground-based and spaceborne observations

P. Saemian[a,*], O. Elmi[a], B. D. Vishwakarma[b], M.J. Tourian[a], N. Sneeuw[a]

[a] *University of Stuttgart, Institute of Geodesy (GIS), Geschwister-Scholl-Str. 24, 70174 Stuttgart, Germany*
[b] *Bristol Glaciology Center, School of Geographical Sciences, University of Bristol, University Road, Bristol BS8 1SS, UK*

Abstract

Lake Urmia, located in the northwestern of Iran, was once the most extensive permanent hypersaline lake in the world. It has been shrinking at an alarming rate during the last two decades. Unsustainable water management in response to increasing demand together with climatic extremes have given rise to the lake's depletion. Based on research findings, short- and long-term approaches have been proposed to revive the lake. The Urmia Lake Restoration Program (ULRP) was established in 2013 aims to restore the lake within a 10-year program. The goal of this paper is to monitor these restoration endeavours over the last six years using spaceborne and ground-based observations. We analysed in-situ water level, surface water extent, and lake water volume of the lake. Water storage change of the Urmia Lake catchment is quantified using the Gravity Recovery and Climate Experiment (GRACE) and GRACE Follow-On satellite observations, which gives us a holistic view of hydrological components in the Lake Urmia basin. Our analysis shows a positive trend of 14.5 cm/year, 204 km^2/year, and 0.42 km^3/year in the time series of lake water level, lake wa-

*Corresponding author: peyman.saemian@gis.uni-stuttgart.de

ter area, and water volume of the lake from 2015 to 2019 which indicates a short-lived stabilization of Lake Urmia over 2015–2019. This has been achieved mainly due to an increase of 0.35 km^3/year in inflow from rivers to the lake, predominantly driven by anomalous precipitation events in 2016 and early 2019. The stabilization seems to be fragile however, since most of the increase in water volume of the lake has spread over the large shallow southern region with high evaporation potential during hot seasons. Furthermore, due to high correlation between lake water level and precipitation, the recovery symptom observed in 2016 and the first half of 2019 might not continue in case of a longer drought period.

Keywords: Lake Urmia, Restoration, Spaceborne observation, Lake desiccation, GRACE-FO

1. Introduction

Lake Urmia, once the largest permanent hypersaline lake in the world, has been shrinking at an alarming rate during the last two decades (Wurtsbaugh et al., 2017; UNEP, 2012). The lake water level and its area have decreased at a rate of 34 cm/yr and 220 km^2/yr, respectively (Tourian et al., 2015). Unsustainable water management in collaboration with increasing demand and climatic extremes have given rise to the observed depletion of the lake (Schulz et al., 2020; AghaKouchak, 2015; Arkian et al., 2018; Ghale et al., 2018; Chaudhari et al., 2018; Shadkam et al., 2016). Precipitation and water inflow from different rivers are the main sources of water into the lake. Precipitation has decreased moderately between -9 mm/year and -20 mm/year while the air temperature of the region has risen significantly between 0.15 °C/year and 0.2 °C/year (Arkian et al., 2018; Nourani et al., 2018; Delju et al., 2013; Fathian et al., 2015). The decrease in rainfall after 1995 played an important role in the documented decline of the lake water level (Arkian et al., 2018). Moreover, the increase in temperature, accompanied by a rise in sunshine duration, has accelerated the rate of evaporation over the lake which is the only direct sink (Nourani et al., 2018).

Many studies have identified various anthropogenic factors responsible for the lake's shrinkage. In particular, the expansion of irrigated land areas and, in consequence, increased water demand for agricultural purposes is one of the main drivers (Shadkam et al., 2016; Alizadeh-Choobari et al., 2016; Ghale et al., 2017; Chaudhari et al., 2018; Khazaei et al., 2018). Moreover, irrigation systems in the catchment often have low efficiency which accounts for significant amount of water loss in the agricultural sector (Dariane & Eamen, 2017). Flow regulation through the construction of dams has decreased the inflow to the lake indirectly by accelerating the irrigation expansion (Shadkam et al., 2016; Hassanzadeh et al., 2012). During two major drought periods, 1997–1998 and 2007–2008, agriculture practices put stress on groundwater resources of the basin by over-extracting water from wells. Tourian et al. (2015) demonstrated that groundwater depletion was alarming between 2003 and 2014, in which the total water storage over the catchment decreased at a rate of about -26.9 ± 18 mm/yr. Similar trend values have been reported by other studies (Voss et al., 2013;

Joodaki et al., 2014; Forootan et al., 2014). Although the studies mentioned above employed different approaches to investigate the main reasons behind the desiccation of the lake, they all found that human intervention was a more significant factor than climate change.

The desiccation of Lake Urmia has threatened the local population's health and economy and raised national and international concern. Based on research findings, short and long-term approaches have been proposed to revive the lake from what was called the *water bankruptcy* (Madani et al., 2016). Revising the surface water management, improving the efficiency of the irrigation systems, introducing a water market, increasing public awareness to conserve water and averting new dam construction are the main strategies that have been advocated (Hassanzadeh et al., 2012; Alizadeh-Choobari et al., 2016; Dariane & Eamen, 2017; Shadkam et al., 2016; Ghale et al., 2018). The government of Iran established the *Urmia Lake Restoration Program*, ULRP, a ten-year program (2013–2023) to revive Lake Urmia in three phases: i) stabilizing the current status; ii) restoration; and iii) sustaining the restoration. The ULRP aims to achieve its objectives by reducing the amount of water required for irrigation within a five-year program. Meanwhile, it plans to boost the water productivity up to 60 % using advanced irrigation systems. Moreover, it is intended to divert water from the Zab and Silveh rivers to the Urmia Lake basin. Finally, the ULRP has planned to use treated waste-water as a source of inflow to the lake.

In the recent past, only a few studies have assessed the progress of the restoration program. Sima et al. (2020) concluded that the ecological water level should be set to a higher level to reduce salinity for recovering brine shrimp and flamingos. Moreover, they suggested defining a range of water level instead of a single ecological level to include more ecosystem services. Danesh-Yazdi & Ataie-Ashtiani (2019) assessed the status of the lake by analyzing its water level over the past six years. They claimed that the current restoration plan needs to be revisited and they highlighted the importance of data for a more realistic model and plan.

In this study, we aim to monitor and analyze the restoration progress of the Lake Urmia using mainly the observations from satellites accompany with ground-based measurements. Furthermore, we discuss the cause of the variation in the status of the lake using hydrological parameters over the lake and its closed basin, including fluxes namely precipitation and evaporation. We present the time series of total water storage (TWS) change of the Urmia basin from the Gravity Recovery and Climate Experiment (GRACE) mission added with its successor GRACE Follow-On for the first time. The ground-based data available for the Urmia basin and the lake includes in situ data of the inflow to the lake, and in situ groundwater data both for validation and analyses. Using the data mentioned above, we have investigated the role of climate factors and human activities, including the ULRP in the region, specifically after 2013.

2. Study area

Lake Urmia, located in northwestern Iran, is one of the world's largest permanent hypersaline lakes and the largest in the Middle East (Figure 1). About

17 permanent and 12 seasonal rivers, as well as a few submarine streams and springs, bring water into the lake. The majority (about 75 %) of the water inflow to the lake comes from river discharge while surface water runoff, groundwater resources, and precipitation provide about 25 % of the water inflow (Eimanifar & Mohebbi, 2007; Zarghami, 2011). Around 41 reservoirs have been constructed over rivers inside the basin since 1970 with the capacity of storing $2 \cdot 10^9\,\mathrm{m}^3$ of water. The surface area of the lake has varied between 1000 and 6000 km^2 during the last two decades (Tourian et al., 2015; Zarghami, 2011). A 1709 m causeway called Shahid Kalantari divided the lake into a northern and a southern part in 2008. Water exchanges between these two part via a culvert along the causeway.

Lake Urmia is located in a closed basin with a catchment area of about 52 000 km^2. In terms of topography, the basin is surrounded by mountains (about 65 % of the catchment area) with vast agriculturally productive plains (about 21 % of the catchment area) located in the middle of the basin and around the lake. The lake and its surrounding area account for nearly 14 % of the total area of the catchment. The altitude of the basin varies between 1280 m and 4886 m above sea level. The basin climate is classified as arid to semi-arid where agriculture depends vitally on irrigation. Based on data from 1973 to 2011, the average annual precipitation over the basin is 352 mm (Farajzadeh et al., 2014). The air temperature of the basin usually varies from 0 to -20° C during the winter period and increases up to 40° C in a hot summer (Eimanifar & Mohebbi, 2007).

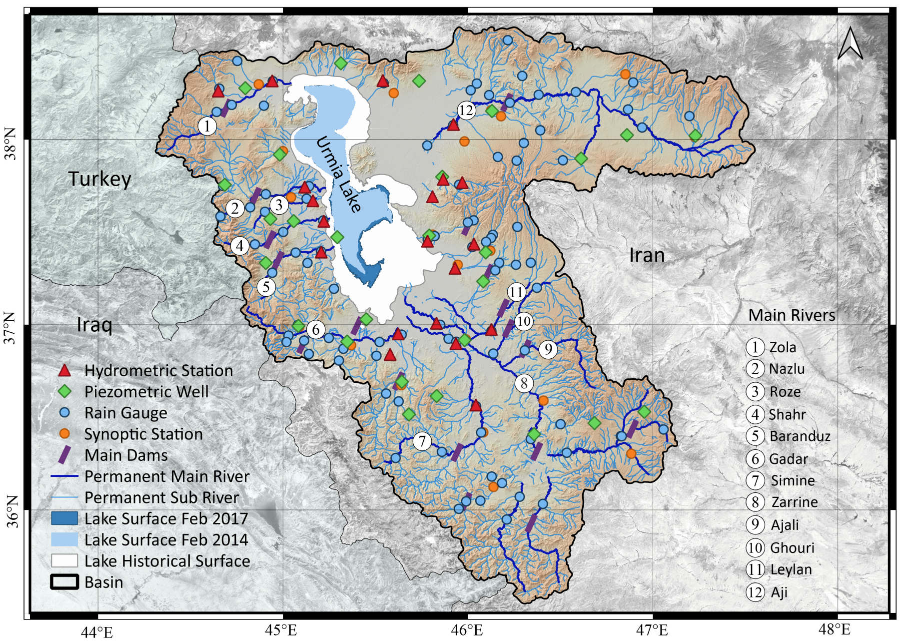

Figure 1: Lake Urmia basin including the main rivers, ground-based stations.

3. Restoration program

The Urmia Lake Restoration Program (ULRP) was established in October 2013. It consists of 6 technical committees and 20 working teams that aim to implement integrated approaches for catchment management and to provide solutions to restore the Urmia Lake (ULRP, 2015b). ULRP has defined its main mission as *Urmia Lake Restoration* and aims to increase the lake water level to reach a so-called *ecological equilibrium* till 2023. The corresponding ecological water level, 1274.67 m above sea level, was established based on water quality conditions (240 $\mathrm{g\,l^{-1}}$ of NaCl) needed to retain brine shrimp *Artemia* (Abbaspour & Nazaridoust, 2007). Three main visions have been announced by ULRP including the life cycle revival of the lake (the most important), integrated water resource management of its basin, and sustainable agricultural development. Moreover, the minimum water level of 1271.72 m, so called health threshold, is crucial to minimize the health risk from dust-prone regions of the lake (Sima et al., 2020; Mardi et al., 2018). This new criterion will assure that more than 90 % of the dust producing areas will be covered with water (RSRC, 2016).

To restore the lake, ULRP has determined three main phases within a ten-year program (ULRP, 2015a):

1. Stabilization (2014–2016)
2. Restoration (2017–2022)
3. Final restoration (2023)

In the first phase, ULRP aimed at maintaining a minimum lake water level and decrease the possible adverse effects of the dried part of the lake like dust storms. The second phase is dedicated to fulfilling the entire lake water demand and gradually increasing the lake level. Finally, in the third phase, ULRP aims to stabilize the water level at the ecological level.

4. Data and methodology

4.1. Data

Evapotranspiration: Only one active actual evapotranspiration monitoring station exists in the basin, located in the eastern part of the Urmia Lake.

The food and agriculture organization of the united nations (FAO) in cooperation with the ULRP has installed some stations since 2019. However, the measurements have not yet been publicly released. The lack of a network of evapotranspiration monitoring stations in the basin and the complexity of a physically-based approach for estimating actual evapotranspiration led us to use global evapotranspiration products. Among global estimates of evapotranspiration, we use the latest product of the European Centre for Medium-Range Weather Forecasts (ECMWF) atmospheric reanalyses of the global climate called ERA5 (Hersbach, 2018) from Copernicus Climate Change Service Climate Data Store (CDS)(`https://cds.climate.copernicus.eu`, last access 25 January 2020). The ECMWF products has shown compatibility with other hydrological data in the region (Lorenz et al., 2014). It should be mentioned that throughout this paper, evapotranspiration means *actual* evapotranspiration and not other sorts like potential or crop evapotranspiration.

Precipitation: Observation from a dense network of rain-gauges provides the best estimation of precipitation over a region. However, in many countries like Iran, recent measurements are not provided publicly. As a result, in this study, we evaluate the performance of 10 gridded precipitation datasets over the Urmia basin compared with a gridded in-situ data from 255 stations. Finally, we selected six bias-corrected datasets and used them for monitoring and assessments. The process of computing gridded precipitation from point measurements and then evaluating the datasets are discussed in detail in AppendixA.

In-situ data: In this study, we include ground water level observations from a network of 1160 piezometric wells from 2002 to the middle of 2017. Moreover, to obtain a better understanding of water resource management inside the basin, we use the time series of water inflow to the lake from rivers and reservoirs from 1995 to the end of 2019. Furthermore, we utilize the in-situ water level of the lake from 1965 to 2019, investigating the long-term change of water level of the lake as well as quantifying the accuracy of satellite altimetry.

Table 1: Summary of all datasets and sensors used in this study.

Variable	Dataset	Resolution		Time period
		Spatial	Temporal	
Precipitation	PRECL	0.5°	1 mo	1948–2019
	CPC	0.5°	1 mo	1979–2019
	GPCP	2.5°	1 mo	1979–2019
	CMAP	2.5°	1 mo	1979–2019
	PERSIANN-CDR	0.25°	1 mo	1983–2019
	CHIRPS	0.05°	1 mo	1981–2019
	ERA5	0.25°	1 mo	1979–2019
	NCEP-1	0.25°	1 mo	1948–2019
	NCEP-2	1.875°	1 mo	1979–2019
	MERRA-2	0.5°	1 mo	1979–2019
Evapotranspiration	ERA5	0.25°	1 mo	1979–2019
Lake area	MODIS (MOD09Q1)	250 m	8 d	2000–2019
Water storage change	GRACE-ITSG-Grace2018	-	1 mo	April 2002–June 2017
	GRACE-FO-ITSG	-	1 mo	June 2018–2019
	WGHM	0.5°	1 mo	1948–2016
Groundwater level	piezometric wells	-	1 mo	2002–2017
Inflow	hydrometric stations	-	1 mo	1995–2019
Water level	water level gauge	-	1 d	1965–2019
Precipitation	rain-gauge	-	1 mo	1965–2013

4.2. Methodology

The surface water extent was obtained using the MODIS surface reflectance 8-day composites with 250 m spatial resolution (MOD09Q1). More than 20 years (2000–2019) MOD09Q1 of data were classified using the ISODATA method (Iterative Self-Organizing Data Analysis Technique). The choice of MODIS over other high-resolution satellite imagery missions like Landsat is due to the need for continuous observation from 2000 to 2019. To quantify the classification uncertainty, we considered all pixels at the lake shoreline and calculated the uncertainty for each area per epoch by

$$\sigma_S = \sqrt{P} \cdot \sigma_{lsa}, \tag{1}$$

where P is the number of shoreline pixels, σ_S is the uncertainty for each epoch, and σ_{lsa} is the uncertainty of the area for a MODIS pixel were lsa stands for lake surface area. We took $0.0625\,\text{km}^2$ which is the maximum value for σ_{lsa}. In order to obtain water volume of the lake, we used in-situ water level and the look-up table for Urmia Lake's level-area-volume relation from Arabsahebi et al. (2019) (Table 7). This look-up table is obtained from the bathymetry map provided by the Water Research Institute (WRI) from a field operation in May 2013 (Arabsahebi et al., 2019).

We employed satellite gravimetry to track total water storage change, in particular GRACE and the GRACE-FO level 02 products (spherical harmonic coefficients up to degree 96) provided by ITSG, Graz (Mayer-Gürr et al., 2018). The C_{20} coefficient in these GRACE fields is replaced by the C_{20} coefficient derived from SLR (Cheng et al., 2013). The degree-1 coefficients were added to the GRACE fields, as suggested by Swenson et al. (2007). Since the GRACE fields are noisy, we use a Gaussian filter of half-width radius 400 km to filter them

(Devaraju, 2015). Then we compute the regional average of total water storage change over the Urmia basin for each month to obtain a time-series. This time-series is not an accurate representation of the hydrological changes because filtering damages the signal via leakage and attenuation (Vishwakarma et al., 2016). To correct for the signal loss, we use the data-driven method of deviation, which has been shown to restore the lost signal to a large extent for small catchments also (Vishwakarma et al., 2017, 2018). In Figure 11 we have plotted the time-series from filtered GRACE fields and the corrected time-series.

5. Results and discussion

To obtain a holistic assessment of the current status of the lake, we present the results and discussions in three parts. First, we investigate the recent water change of the lake by monitoring and analysing the water level, surface area, and volume of the lake. In the second part, we study the water balance in Lake Urmia as an independent system (see figure 2a). In this part, we assess the time series of precipitation and lake inflow as the sources and evaporation as the only sink. Finally, we investigate changes in the main parameters of the basin, including the water balance fluxes (see figure 2b).

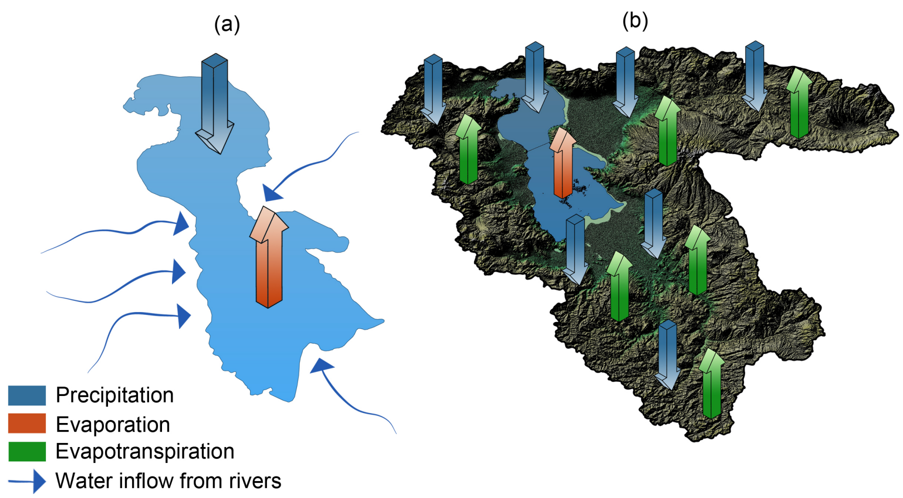

Figure 2: Schematic diagram of the water balance for (a) Lake Urmia, and (b) Lake Urmia basin.

5.1. Monitoring the lake's water change

Lake water level

Figure 3 (a) shows the 55-year time series of daily in-situ lake water level from 1965 to 2019. The long-term water level puts our comparison between the last two decades, especially the last six years, into perspective with the former state of the lake in the last three decades of the twentieth century. The water level dropped by more than 8 m during 1995–2015. Since October 2002, the lake has never seen its ecological water level. The reasons behind this noticable decline in lake water level have been discussed in previous studies (e.g., Schulz et al. (2020); Khazaei et al. (2018); Ghale et al. (2018); Chaudhari et al. (2018)).

The negative trend in the water level has tapered off since late 2015 and early 2016 (Figure 3 (a)). Figure 3 (b) compares the observed lake water level time series with the two main goals of the restoration program, namely the ecological water level and the health threshold, in the time-frame of the restoration program. The result shows that stabilization is achieved but at a lower level than planned. Moreover, the lake level climbed above the health threshold briefly in April 2019. Figure 3 (c) shows the inter-annual change of water level from 2014 to 2019 more elaborately. Lake water level has risen overall from its lowest level from 2015 to 2019. In 2016, the level of the lake increased on average about 40 cm in comparison to 2015, except for the first two months of the year. Although the lake water level decreased by an average of 14 cm and 17 cm cm in 2017 and 2018, respectively, it still was in a better situation than 2015, on average 16 cm and 12.5 cm higher, respectively. In 2019, the lake experienced its highest water level over the past decade. In the first seven months of the year, the average water level of the lake was more than 74 cm higher than in 2015, with the average monthly variation this year found to be similar to 2010. The lake experienced a positive trend of 14.5 cm/year from 2015 to 2019. Rainfall was much higher than the average long-term in 2016 and especially in March–May 2019. This increase in rainfall is one of the main reasons for the increase in these two years. The rainfall variations in the basin are investigated in more detail in section 5.3.

Lake surface water extent

Results from the classification of the satellite imagery are shown as time series in Figure 4 (top) together with the in-situ water level measurements. The

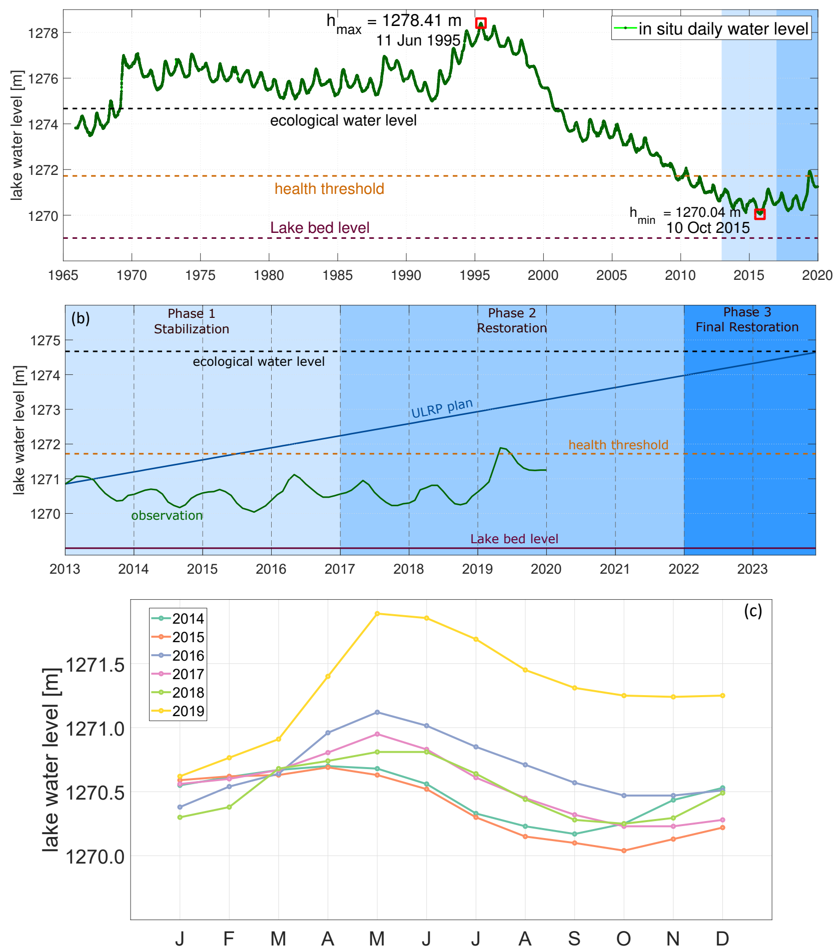

Figure 3: (a) Lake Urmia historical daily in-situ water level from 1965 to 2019; (b) Lake Urmia monthly in-situ water level (in green) compared with the two water level goals of the restoration program, namely ecological water level and health threshold in the time frame of three phase of restoration plan; (c) Monthly in-situ water level from 2014 to 2019.

high correlation between the two time series (0.96) reflects a high consistency. We have evaluated the time series of surface water extent from ISODATA compared with the height-area look-up table presented by Arabsahebi et al. (2019). The result of the evaluation is shown in AppendixB.

From 2015 to the end of 2018, a trend in the lake area is negligible although a large annual amplitude exists. The lake experienced a jump and reached 2922 km^2 in June 2016. The average area of the lake was 1489 km^2 and 1246 km^2 in 2017 and 2018, respectively, which is the same as in 2015, with peaks only slightly higher in the spring. Between the years 2015–2017, Lake Urmia has gained nearly 300 km^2. The water area of the lake in 2019 witnessed a dramatic increase and reached 2407 km^2 on average for the first seven months. This average was last seen in 2011. The MODIS snap-shots of the lake for the 25th of May in different years depict it state (Figure 4, bottom). May is the month in which the lake has shown its highest water level over the last two decades. The area reduction is visible from the year 2006 until 2010 mainly from the southeastern part. From 2010 the lake started to dry almost from all directions to the end of 2015. From 2016 to 2018, under the influence of restoration endeavours, the area starts to expand mainly in the southern half. As discussed above, in the year 2019 the surface area of the lake expanded abruptly and reached a state last seen in 2009–2011. The time series of surface area of the Urmia lake indicates a positive trend of $204 \pm 6\,km^2/yr$ from 2015 to 2019.

In order to obtain a better understanding of the lake area variations during the monitoring period, water coverage frequency maps of Lake Urmia for specific periods are presented in figure 5. Figure 5(a) presents a map of water coverage frequency for the whole monitoring period (2000–2019); divided into four sub-periods in Figure 5(b,c,d, e). The inner part of the lake in the north was the only part with 100 % coverage of water. Considering the early years (2000–2006) as the period with the highest number of pixels with more than 95 %

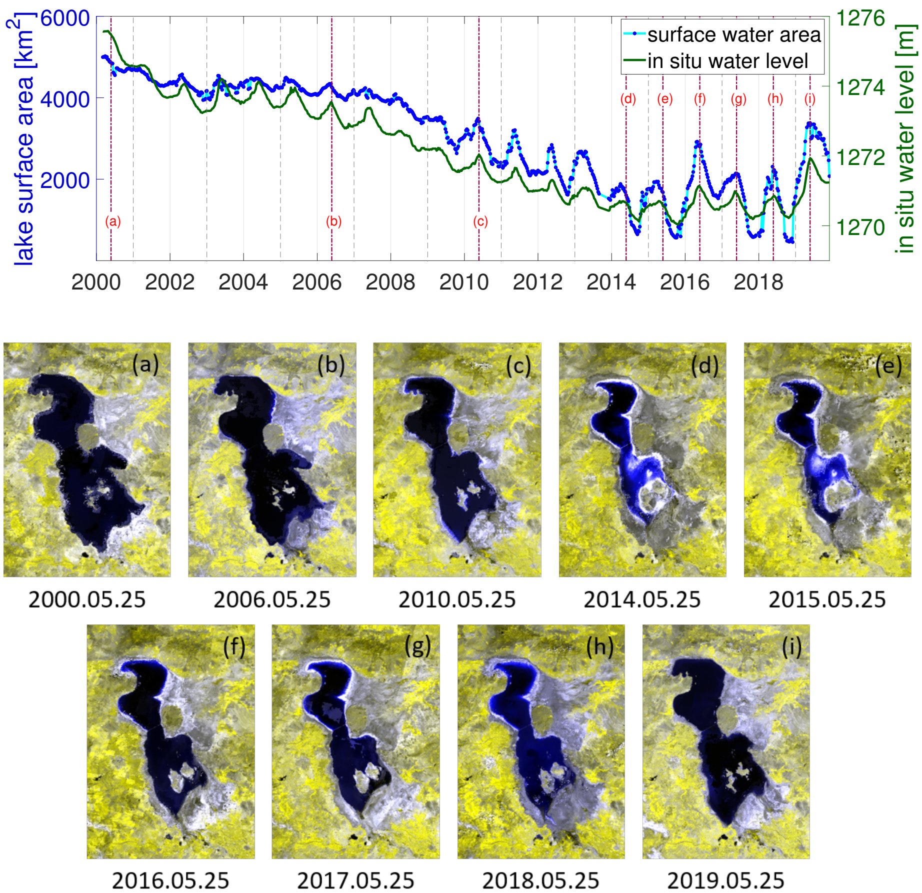

Figure 4: (Top) Time series of surface water extent obtained from MODIS imagery and the time series of in-situ water level from 2000 to 2019; (Bottom) False-color RGB combination of bands 2, 2, and 1 of MODIS MOD09Q1 product over Lake Urmia for selected dates. The position of each of these images is shown in time series. Images including (a), (b), (c), (d), and (e) plotting the desiccation period of the lake and images including (f), (g), (h), and (i) show the restoration period.

water coverage frequency, Figure 5(d and e) shows that the lake was shrinking from the southern part from 2007 to 2014. The vast area of the lake has been covered by the pixels with light blue and green colors indicating the annual cycle in this period. Comparing to the area of the lake in the period of 2011–2014, the lake has expanded from 2015 to 2019, mainly in the southern part. However,

Figure 5(b) shows that this expansion only happened in the less than 20 % of the period, which is clear to be the year 2019.

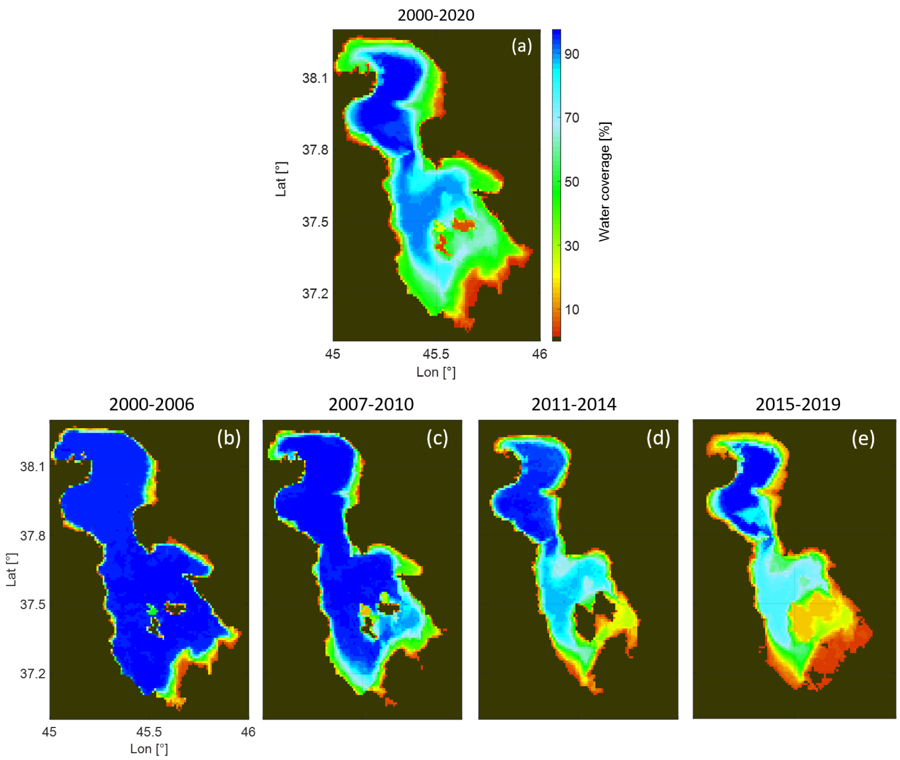

Figure 5: Water coverage frequency maps for Urmia Lake for the last two decades, 2000–2020 (a), and its sub-periods including 2000–2006 (b), 2007–2010 (c), 2011–2014 (d), and the last five years 2015–2019 (e). 100 % and 0 % coverage means being wet and dry, respectively, for the whole time period.

Figure 6a characterizes four main phases for Lake Urmia by plotting the lake surface area versus in-situ water level measurements. The colors (pointedly ordered in traffic light colors) represent different behaviour of the lake's bed. A high slope of the lake bed will led to large changes in the surface water area against slight changes in the lake water level. In this way, yellow dots represent the deepest slope in the lake bed and green dots indicate the mildest slope. The scatter plot delineates the shrinking process of the lake with a weak negative trend in green dots, strong negative trend in yellow and red dots, and positive trend in orange dots. The orange dots depicts water spread over a larger area but with a shallow depth which can accelerate the rate of evaporation from the lake.

To investigate the changes in the lake over the last six years in more detail, we analyze the scatter plot of area versus the in-situ water level of the lake between 2014 to 2019 (shown in Figure 5b). The colors follow Figure 3 (bottom). The year 2014 is included as a reference for tracking the process of desiccation. A clear drop occurred in both surface area and the water level in October 2015, corresponding to the lowest water level of the lake in the last 53 years.

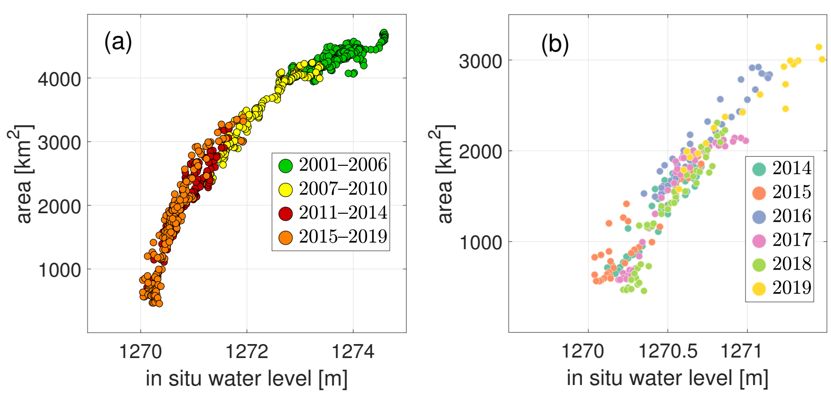

Figure 6: Scatter plot of surface water extent versus water level, a) for four different time periods: 2001–2006, 2007–2010, 2011–2014, and 2015–2018. b) for the six last years 2014–2019.

Lake water volume variation

Figure 7 illustrates the time series of lake volume from 2000 to the end of 2019. The time series has a negative trend of $1.2\,\mathrm{km}^3/\mathrm{yr}$ from 2000 to

2014. From the beginning of 2015 to the end of 2017 the trend is near-zero (0.02 km^3/yr). This can be interpreted as stabilization though at a very low level of around 2 km^3 (9 % of its early 2000s volume). From 2015 to the end of 2019, the time series of water volume of the Urmia lake shows a positive trend of 0.42 km^3/year. The gray inset presents the estimation of the area compared with the volume of the lake within 2015–2019.

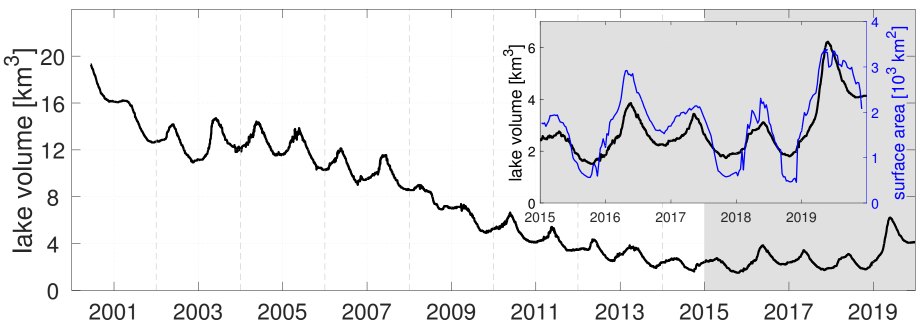

Figure 7: Time series of lake water volume estimated using the look-up table provided by Arabsahebi et al. (2019) and in-situ lake water level

The time series of the lake water level, surface water extent, and water volume confirm a stabilization of the lake between 2016 and 2019. Climate factors such as precipitation, evaporation, and temperature accompanied by the restoration endeavours have contributed positively to achieve a stabilized lake water level. In the next section, we present the result of monitoring the main terms of the water balance for the lake. Isolating the lake and observing water balance terms provides a holistic view of the factors affecting lake level in recent years.

5.2. Investigating sources and sinks

Figure 8 shows the time series of lake volume together with the sources (precipitation (P) and inflow from rivers (Q)) and sink (evaporation(E)) over 2016–2019. Significant correlations between lake volume changes and water balance components indicate the validity of the calculations. Over the last four years, the volume of the lake increased with a trend of $0.43\,\mathrm{km}^3$/year. The evaporation from the lake shows weak positive trend of $0.02\,\mathrm{km}^3$/year and precipitation to the lake $0.10\,\mathrm{km}^3$/year. The total inflow to the lake from rivers increased with a trend of $0.35\,\mathrm{km}^3$/year. Considering these values and the water balance of the lake:

$$P + Q - E = \frac{\mathrm{d}S}{\mathrm{d}t} \tag{2}$$

where S is the water volume of the lake, one can conclude that the main cause of the increase in water volume of the lake comes from the change in the inflow from rivers. We monitored the ratio of inflow to the total precipitation of the Urmia basin over the last 25 years back to 1995 when the lake had its highest area. The precipitation shows a positive trend from 1995 to 2019, ignoring the inter-annual fluctuations of precipitation to the basin. Although the basin gained more water in the 2000s and 2010s, the inflow from rivers declined. This decline is correlated with the decrease in the water volume of the lake and acknowledged in the previous studies like (Danesh-Yazdi & Ataie-Ashtiani, 2019; Schulz et al., 2020). From 2015, with initiating the restoration endeavours in the basin, the lake gained more water from rivers and reservoirs as the inflow which is highly correlated with the rise in the water volume of the lake.

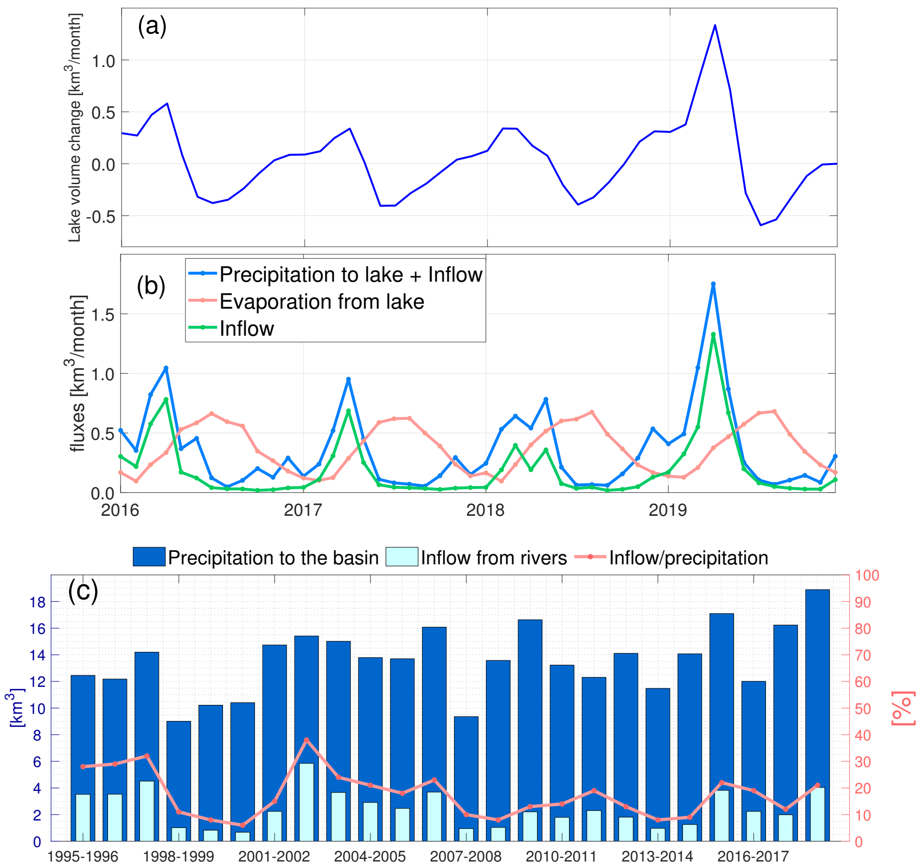

Figure 8: (a) Time series of lake volume change and (b) precipitation to the lake, evaporation from the lake, and the total inflow to the lake from rivers from 2016 to 2019, all in monthly time step. (c) Bar graph of average monthly precipitation to the basin (excluding lake) and inflow to the lake. The ratio between inflow to the lake and the precipitation to the basin is shown in percentage using the right vertical axis.

Lake Urmia lies at the lowest point in a closed drainage basin. Natural and anthropogenic activities inside the basin affect the state of the lake. Therefore, we monitored the water balance fluxes, namely precipitation and evapotranspiration, in section 5.3. Water balance fluxes consider surface water change and are blind to the deep groundwater change. Hence we employed GRACE to monitor total water storage change inside the catchment (see section 5.3).

5.3. Urmia catchment

In this section, we investigate the change in the components of the water balance of the Urmia basin, namely precipitation, evapotranspiration, and the total water storage anomaly. These parameters have been surveyed to understand the reasons behind the desiccation of the lake (Arkian et al., 2018; Ghale et al., 2018; Shadkam et al., 2016; Tourian et al., 2015). Precipitation represents more natural variation in the climate, while anthropogenic activities like agriculture can influence evapotranspiration. Finally, satellite gravimetry provides a holistic view of storage change in the basin, including variation in deep water. Expansion of irrigated area is reported as a primary cause of the lake's desiccation (Khazaei et al., 2018; Schulz et al., 2020). However, monitoring and analysing the spatio-temporal change of the agricultural land area needs ground-based observations for calibration and validation. Since such an observation is not available for the restoration period, we have not included an assessment of irrigated area into our analyses.

Water balance fluxes

Figure 9 demonstrates the time series of three month time-scale Standardized Precipitation Index (SPI; (McKee et al., 1993)) from 1983 to 2019. Different classes of wetness and dryness are displayed in the legend of Figure 8. In the past four decades, the catchment has mostly experienced an equal number of dry and wet years in each decade though with different intensity. The average precipitation were 301, 299, 292, and 293 mm/year over the 1980s, 1990s, 2000s, and 2010s, respectively. However, in the course of the late 1990s and mid-2000s, the severity and frequency of droughts increased, leading to a strong reduction in lake levels. By the start of the restoration endeavours in 2015, the basin experienced more often a wet condition (25 %) than dry (only 5 %) of the period from 2015 to 2019. Over the last 45 months (70 %) the basin varied between mildly wet to mildly dry.

Figure 10 shows monthly, and average annual lake water level together with the monthly time series of basin-wide precipitation and evapotranspiration from 2014 to 2019. A positive recharge ($P - ET$) occurred in 2015, 2016, 2018, and 2019. The positive recharge in 2015 and 2018 happened after a year of negative recharge which helped the basin to recover. The same amount of positive recharge in 2016 and 2019, equivalent to about $800 \times 10^6\,\mathrm{m}^3$ water, led to different amounts of increase in water level. This can be explained by the double amount of water that has been released to the lake in 2019 relative to 2016 (see Figure 8). The precipitation over the basin indicates a moderate positive trend of $0.65\,\mathrm{km}^3$/year) while evapotranspiration shows a weak positive trend of $0.20\,\mathrm{km}^3$/year) from 2015 to 2019. As a result, the basin is recharged trend-wise at a level of about $0.40\,\mathrm{km}^3$/year. Therefore the positive trend in the water volume of the lake is largely obtained by an interchange of water from reservoirs and rivers to the lake, instead of being used in the agricultural lands.

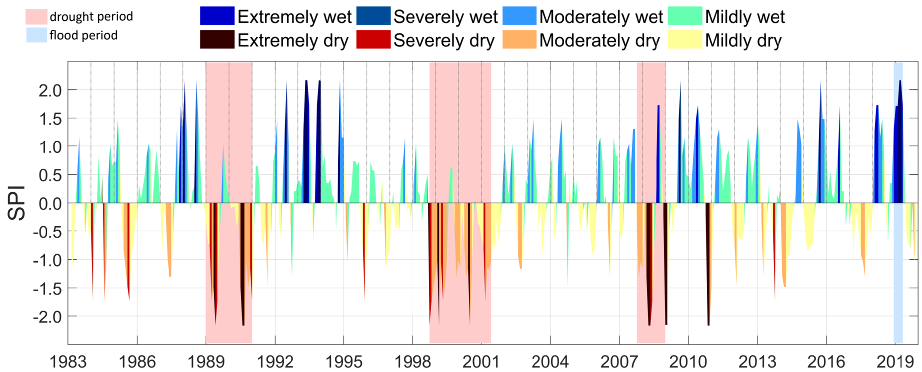

Figure 9: Three month time scale of SPI over the Urmia basin from 1983 to 2019. The categories of wetness and dryness are shown for each month with the corresponding color in the legend.

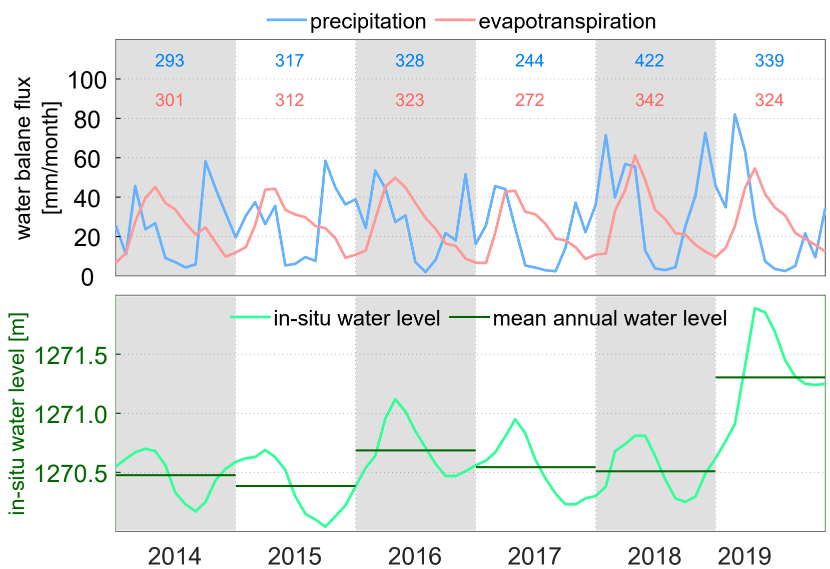

Figure 10: Top: Inter-annual variation of precipitation and evapotranspiration over the catchment including total annual precipitation (blue numbers) and evapotranspiration (red numbers); bottom: Lake water level from 2014 to 2019.

Water storage

Figure 11(a) shows water storage variations in terms of equivalent water height over the Lake Urmia basin for the time period of GRACE and GRACE-FO (2003–2019), compared with WGHM (2003–2016). The total water storage change time series from GRACE and WGHM follow each other well but peak-to-peak amplitude are different for the time period 2003–2008. The long-term behaviour of WGHM does not follow the GRACE observations after 2008. The disagreement is likely due to the fact that WGHM model assumes no change in the arable area in Iran over the years, while the area of agricultural land did increase. The model uses estimates of arable land from the Food and Agricultural Organization of the UN that does not provide recent estimates of irrigated area in Iran (see http://www.fao.org/nr/water/aquastat, last accessed: 13 Feb. 2018).

For each piezometric well, we have subtracted the mean and normalized it by its standard deviation. Then we averaged the normalized groundwater at each month over the basin. Finally, we multiplied back the mean of standard deviation values at each month to reach the time of mean groundwater of the basin. The time series of storage change obtained from GRACE matches well with the time series of the mean groundwater level from piezometric wells data. Please note the steep change observed in the 2007–2008 drought (cf. Figure 11 b). For further validation, we assess the agreement between $P - ET$ and GRACE in the water balance equation:

$$P - ET = \frac{\mathrm{d}M}{\mathrm{d}t} \tag{3}$$

The GRACE rate of water storage changes $\mathrm{d}M/\mathrm{d}t$ matches with recharge $(P - ET)$ relatively well with a correlation coefficient of 0.86 (Fig. 11 c). We utilize singular spectrum analysis (SSA) first to extract the non-linear trend from the GRACE water storage change time series and then fit a line to obtain linear trend (Chen et al., 2013). A window of 24 months is used to extract the non-linear trend. The TWS decays at a rate of 24 ± 0.4 mm/year between 2003 and 2015. The linear trend seems to be negligible from 2015 to 2017 indicating stabilization of the TWS change. In other words the water storage of the Urmia basin seems to reach a new equilibrium. The result from GRACE-FO from June 2018 to the end of 2019 shows a positive trend in the TWS which is correlated with the water recharge in Figure 11(c).

The volume of the lake increased by $0.43\,\mathrm{km}^3$/year from 2016 to 2019. The TWS increase at a rate of 14 ± 0.8 mm/year over the same period, ignoring the gap from July 2017 to May 2018. By multiplying the trend of equivalent water height with the area of the basin (51,931 km^2), we obtain a water volume gain of about $0.72 \pm 0.04\,\mathrm{km}^2$/year over the whole basin. The difference between the water volume gain from satellite gravimetry and volume of the lake indicates recharge of the groundwater over the last four years.

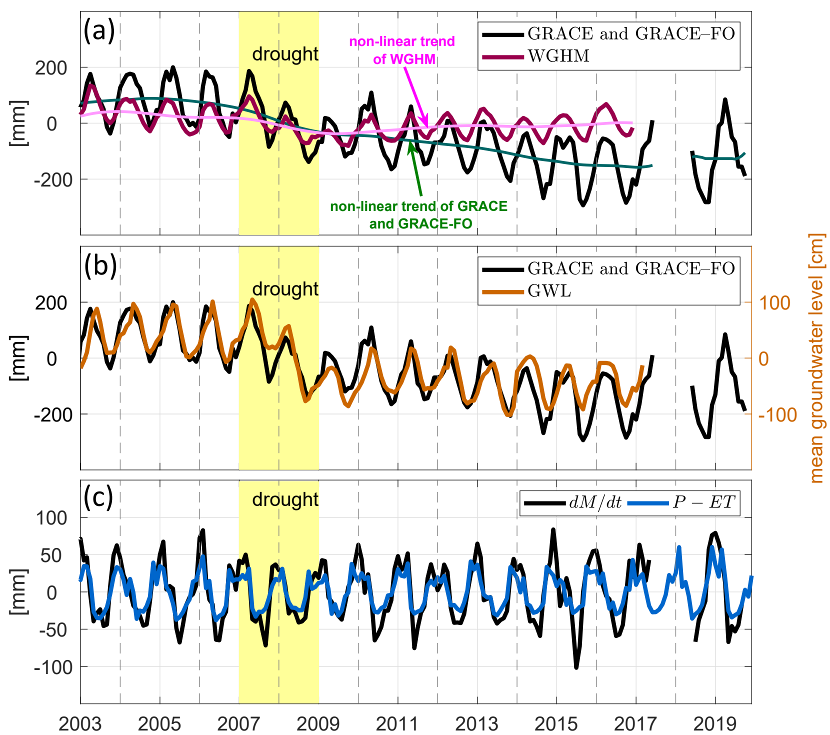

Figure 11: (a): Total water storage change over Lake Urmia basin from GRACE and GRACE–FO, compared with WGHM. (b): Total water storage change over Lake Urmia basin from GRACE and GRACE–FO, compared with mean groundwater level from piezometric wells. (c): GRACE and GRACE–FO rate of water storage changes together with corresponding recharge ($P - ET$). In all panels the 2007–2008 drought period is shown with a yellow background.

6. Conclusion

Lake Urmia, one of the world's largest saline lakes in northwestern Iran, has endured two decades of desiccation due to both climate factors and improper water management. This led to setting up the *Urmia Lake Restoration Program* in 2013, which has been actively trying to stabilize the lake since 2014 and restoring the lake's water level to the ecological level of 1274.67 m within ten years of its establishment. Although numerous attempts have been made to investigate the reasons behind the lake desiccation, very few studies have assessed the state of the lake after the restoration endeavours started. Monitoring the efficacy of the lake restoration program while understanding the drivers of change in the lake is a challenging task. In this study, we demonstrate that spaceborne observations, together with ground-based measurements can help us to monitor the efficacy of the restoration efforts. Based on our results, we can conclude that:

- Lake Urmia was stabilized from 2015 to 2019. Positive trends of 14.5 cm/year, $204\,\mathrm{km}^2$/year, and $0.42\,\mathrm{km}^3$/year are observed in the time series of lake water level, lake water area, and water volume of the lake.

- The time series of precipitation does not show any significant trend between 2015–2018. To be more precise, except for 2017 (two months with moderate drought) and 2016 (moderately wet), all years were conform with the long-term climatology of the catchment. However, the catchment received massive water from heavy rainfall in spring 2019. Experiencing such a drought-free period from 2015 to 2019 significantly helped stopping the shrinkage of the lake and push it into the restoration phase.

- The water balance of the Lake Urmia shows that about 80 % of the rise in water volume of the lake since 2015 is caused by the positive trend in the inflow from rivers and reservoirs. The remainder is due to the increase in the precipitation to the lake itself.

- The positive trend in the recharge ($P - ET$) of $0.40\,\mathrm{km}^3$/year on the one hand and the positive trend in the water volume of the lake on the other hand imply that the lake has benefited from a significant portion of water that is not used for agricultural purpose but released to the lake instead.

- The water storage shows no significant decrease from 2015 to the end of 2017 and an overall increase of 26 ± 5 mm since 2019. The new state of the water storage and water fluxes of the Urmia basin is comparable with the state around 2010–2012.

- Considering the trend of precipitation, lake surface area, inflow to the lake, and evaporation from the catchment, the first phase of restoration program is accomplished at the cost of releasing water from reservoirs.

- The stabilization seems to be fragile however, since most of the increase in water volume of the lake has spread over the large shallow region in the south with high evaporation potential during hot seasons. Furthermore, due to high correlation between lake water level and precipitation, the recovery step observed in 2016 and the first half of 2019 might not continue in case of a longer drought period.

The results of this study are in line with studies in recent years, which generally analyzed Lake Urmia's desiccation (Hosseini-Moghari et al., 2018; Khazaei et al., 2018; Chaudhari et al., 2018; Ghale et al., 2018). In order to achieve a sustainable restoration, more tenable efforts are required, such as those suggested in previous studies including preventing diversion of water flows into the lake towards agricultural land. Our result showed that the Lake Urmia had been stabilized as the result of a largely positive trend in the inflow to the lake, mainly due to the heavy rainfall in 2019. Since the elevation of Lake Urmia in the southern part is associated with shallow water depths, the process of lake restoration might not be sustainable and is feared to be reversed by drought in the coming years.

Conflict of Interests

The authors declare that there is no conflict of interests regarding the publication of this paper.

Acknowledgment

The authors would like to thank Dr. Behdad Chehrehnegar, the head of the department of hydro-informatics of ULRP, and Hamid Farahmand, research scientist at ULRP for their kind assistance in sharing the lake water level data and inflow from hydrometric stations including release from reservoirs. The authors acknowledge the Copernicus Climate Change Service (C3S), Princeton University, the NASA/Goddard Space Flight Center, and the University of Frankfurt for producing and making available the datasets of ERA5, MSWEP, TRMM, and WGHM, respectively. The ENVISAT and CryoSat-2 data were provided by the European Space Agency and MODIS products from MODIS land team validation site. Peyman Saemian acknowledge the Sustainable Water Management–NaWaM program from the Federal Ministry of Education and Research (BMBF) and the German Academic Exchange Service (DAAD) for the support for his PhD grant. Bramha Dutt Vishwakarma is now supported by the Marie Skłodowska-Curie Individual fellowship (MSCA-IF) (under grant agreement no 841407 (CLOSeR)). He was until recently supported by the European Research Council (ECR) under the European Union's Horizon 2020 Research and Innovation Program under Grant Agreement 694188, the Global Mass project.

References

Abbaspour, M., & Nazaridoust, A. (2007). Determination of environmental water requirements of Lake Urmia, Iran: an ecological approach. *International Journal of Environmental Studies*, *64*, 161–169. doi:10.1080/00207230701238416.

Adler, R. F., Huffman, G. J., Chang, A., Ferraro, R., Xie, P.-P., Janowiak, J., Rudolf, B., Schneider, U., Curtis, S., Bolvin, D. et al. (2003). The version-2 global precipitation climatology project (GPCP) monthly precipitation analysis (1979–present). *Journal of hydrometeorology*, *4*, 1147–1167. doi:10.1175/1525-7541(2003)004<1147:tvgpcp>2.0.co;2.

AghaKouchak, A. (2015). Recognize anthropogenic drought. *Nature*, *524*, 409. doi:10.1038/524409a.

Alizadeh-Choobari, O., Ahmadi-Givi, F., Mirzaei, N., & Owlad, E. (2016). Climate change and anthropogenic impacts on the rapid shrinkage of Lake Urmia. *International Journal of Climatology*, *36*, 4276–4286. doi:10.1002/joc.4630.

Arabsahebi, R., Voosoghi, B., & Tourian, M. J. (2019). A denoising–

classification–retracking method to improve spaceborne estimates of the water level–surface–volume relation over the Urmia Lake in Iran. *International Journal of Remote Sensing*, (pp. 1–28). doi:10.1080/01431161.2019.1643938.

Arkian, F., Nicholson, S. E., & Ziaie, B. (2018). Meteorological factors affecting the sudden decline in lake Urmia's water level. *Theoretical and Applied Climatology*, *131*, 641–651. doi:10.1007/s00704-016-1992-6.

Ashouri, H., Hsu, K.-L., Sorooshian, S., Braithwaite, D. K., Knapp, K. R., Cecil, L. D., Nelson, B. R., & Prat, O. P. (2015). PERSIANN-CDR: Daily precipitation climate data record from multisatellite observations for hydrological and climate studies. *Bulletin of the American Meteorological Society*, *96*, 69–83. doi:10.1175/BAMS-D-13-00068.1.

Chaudhari, S., Felfelani, F., Shin, S., & Pokhrel, Y. (2018). Climate and anthropogenic contributions to the desiccation of the second largest saline lake in the twentieth century. *Journal of Hydrology*, *560*, 342–353. doi:10.1016/j.jhydrol.2018.03.034.

Chen, M., Xie, P., Janowiak, J. E., & Arkin, P. A. (2002). Global land precipitation: A 50-yr monthly analysis based on gauge observations. *Journal of Hydrometeorology*, *3*, 249–266. doi:10.1175/1525-7541(2002)003<0249:GLPAYM>2.0.CO;2.

Chen, Q., van Dam, T., Sneeuw, N., Collilieux, X., Weigelt, M., & Rebischung, P. (2013). Singular spectrum analysis for modeling seasonal signals from GPS time series. *Journal of Geodynamics*, *72*, 25–35. doi:10.1016/j.jog.2013.05.005.

Cheng, M., Tapley, B. D., & Ries, J. C. (2013). Deceleration in the Earth's oblateness. *Journal of Geophysical Research: Solid Earth*, *118*, 740–747. doi:10.1002/jgrb.50058.

Danesh-Yazdi, M., & Ataie-Ashtiani, B. (2019). Lake Urmia crisis and restoration plan: planning without appropriate data and model is gambling. *Journal of Hydrology*, *576*, 639–651. doi:10.1016/j.jhydrol.2019.06.068.

Dariane, A. B., & Eamen, L. (2017). Finding the causes and evaluating their impacts on Urmia lake crisis using a comprehensive water resources simulation model. *Journal of Hydraulic Structures*, *3*, 62–77. doi:10.22055/jhs.2018.24762.1064.

Delju, A., Ceylan, A., Piguet, E., & Rebetez, M. (2013). Observed climate variability and change in Urmia lake basin, Iran. *Theoretical and applied climatology*, *111*, 285–296. doi:10.1007/s00704-012-0651-9.

Devaraju, B. (2015). *Understanding filtering on the sphere – Experiences from filtering* GRACE *data*. Ph.D. thesis Universität Stuttgart. URL: elib.uni-stuttgart.de/bitstream/11682/4002/1/BDevarajuPhDThesis.pdf.

Eimanifar, A., & Mohebbi, F. (2007). Urmia lake (northwest Iran): a brief review. *Saline systems*, *3*, 5. doi:10.1186/1746-1448-3-5.

Farajzadeh, J., Fard, A. F., & Lotfi, S. (2014). Modeling of monthly rainfall and runoff of Urmia lake basin using "feed-forward neural network" and "time series analysis" model. *Water Resources and Industry*, *7*, 38–48. doi:10.1016/j.wri.2014.10.003.

Fathian, F., Morid, S., & Kahya, E. (2015). Identification of trends in hydrological and climatic variables in Urmia Lake basin, Iran. *Theoretical and Applied Climatology*, *119*, 443–464. doi:10.1007/s00704-014-1120-4.

Forootan, E., Rietbroek, R., Kusche, J., Sharifi, M., Awange, J., Schmidt, M., Omondi, P., & Famiglietti, J. (2014). Separation of large scale water storage patterns over Iran using GRACE, altimetry and hydrological data. *Remote Sensing of Environment*, *140*, 580–595. doi:10.1016/j.rse.2013.09.025.

Funk, C., Peterson, P., Landsfeld, M., Pedreros, D., Verdin, J., Shukla, S., Husak, G., Rowland, J., Harrison, L., Hoell, A. et al. (2015). The climate hazards infrared precipitation with stations—a new environmental record for monitoring extremes. *Scientific data*, *2*, 150066. doi:10.1038/sdata.2015.66.

Ghale, A., Baykara, M., & Unal, A. (2017). Analysis of decadal land cover changes and salinization in Urmia lake basin using remote sensing techniques. *Nat. Hazards Earth Syst. Sci. Discuss.*, . doi:10.5194/nhess-2017-212.

Ghale, Y. A. G., Altunkaynak, A., & Unal, A. (2018). Investigation anthropogenic impacts and climate factors on drying up of Urmia lake using water budget and drought analysis. *Water Resources Management*, *32*, 325–337. doi:10.1007/s11269-017-1812-5.

Hassanzadeh, E., Zarghami, M., & Hassanzadeh, Y. (2012). Determining the main factors in declining the Urmia lake level by using system dynamics modeling. *Water Resources Management*, *26*, 129–145. doi:10.1007/s11269-011-9909-8.

Hersbach, H. (2018). *Operational global reanalysis: progress, future directions and synergies with NWP*. European Centre for Medium Range Weather Forecasts.

Hosseini-Moghari, S.-M., Araghinejad, S., Tourian, M. J., Ebrahimi, K., & Döll, P. (2018). Quantifying the impacts of human water use and climate variations on recent drying of Lake Urmia basin: the value of different sets of spaceborne and in-situ data for calibrating a hydrological model. *Hydrology and Earth System Sciences*, . doi:10.5194/hess-2018-318.

Joodaki, G., Wahr, J., & Swenson, S. (2014). Estimating the human contribution to groundwater depletion in the Middle East, from GRACE data, land surface models, and well observations. *Water Resources Research*, *50*, 2679–2692. doi:10.1002/2013WR014633.

Kalnay, E., Kanamitsu, M., Kistler, R., Collins, W., Deaven, D., Gandin, L., Iredell, M., Saha, S., White, G., Woollen, J. et al. (1996). The ncep/ncar 40-year reanalysis project. *Bulletin of the American meteorological Society*, *77*, 437–472.

Kanamitsu, M., Ebisuzaki, W., Woollen, J., Yang, S.-K., Hnilo, J., Fiorino, M., & Potter, G. (2002). NCEP–DOE AMIP-II reanalysis (r-2). *Bul-*

letin of the American Meteorological Society, *83*, 1631–1644. doi:10.1175/bams-83-11-1631(2002)083<1631:nar>2.3.co;2.

Khazaei, B., Khatami, S., Alemohammad, S. H., Rashidi, L., Wu, C., Madani, K., Kalantari, Z., Destouni, G., & Aghakouchak, A. (2018). Climatic or regionally induced by humans? Tracing hydro-climatic and land-use changes to better understand the lake Urmia tragedy. *Journal of Hydrology*, . doi:10.1016/j.jhydrol.2018.12.004.

Lorenz, C., Kunstmann, H., Devaraju, B., Tourian, M. J., Sneeuw, N., & Riegger, J. (2014). Large-scale runoff from landmasses: a global assessment of the closure of the hydrological and atmospheric water balances. *Journal of Hydrometeorology*, *15*, 2111–2139. doi:10.1175/JHM-D-13-0157.1.

Madani, K., AghaKouchak, A., & Mirchi, A. (2016). Iran's socio-economic drought: challenges of a water-bankrupt nation. *Iranian Studies*, *49*, 997–1016. doi:10.1080/00210862.2016.1259286.

Mardi, A. H., Khaghani, A., MacDonald, A. B., Nguyen, P., Karimi, N., Heidary, P., Karimi, N., Saemian, P., Sehatkashani, S., Tajrishy, M. et al. (2018). The Lake Urmia environmental disaster in Iran: A look at aerosol pollution. *Science of The Total Environment*, *633*, 42–49. doi:10.1016/j.scitotenv.2018.03.148.

Mayer-Gürr, T., Behzadpour, S., Ellmer, M., Kvas, A., Klinger, B., Strasser, S., & Zehentner, N. (2018). ITSG-Grace2018–monthly, daily and static gravity field solutions from GRACE, GFZ dataservices. doi:10.1029/2019jb017415.

McKee, T. B., Doesken, N. J., Kleist, J. et al. (1993). The relationship of drought frequency and duration to time scales. In *Proceedings of the 8th Conference on Applied Climatology* (pp. 179–183). American Meteorological Society Boston, MA volume 17.

Nourani, V., Mehr, A. D., & Azad, N. (2018). Trend analysis of hydroclimatological variables in Urmia lake basin using hybrid wavelet Mann–Kendall and şen tests. *Environmental Earth Sciences*, *77*, 207. doi:10.1007/s12665-018-7390-x.

Rienecker, M. M., Suarez, M. J., Gelaro, R., Todling, R., Bacmeister, J., Liu, E., Bosilovich, M. G., Schubert, S. D., Takacs, L., Kim, G.-K. et al. (2011). Merra: Nasa's modern-era retrospective analysis for research and applications. *Journal of climate*, *24*, 3624–3648. doi:10.1175/jcli-d-11-00015.1.

RSRC (2016). *Identification and Prioritization of Dust Sources in Lake Urmia Bed and Its Margin (unpublished report in Farsi)*. Technical Report Remote Sensing Research Center, Sharif University of Technology.

Schulz, S., Darehshouri, S., Hassanzadeh, E., Tajrishy, M., & Schüth, C. (2020). Climate change or irrigated agriculture–what drives the water level decline of Lake Urmia. *Scientific Reports*, *10*, 1–10. doi:10.1038/s41598-019-57150-y.

Shadkam, S., Ludwig, F., van Oel, P., Kirmit, Ç., & Kabat, P. (2016). Impacts of climate change and water resources development on the declining inflow into

Iran's Urmia lake. *Journal of Great Lakes Research*, *42*, 942–952. doi:10.1016/j.jglr.2016.07.033.

Sima, S., Rosenberg, D. E., Wurtsbaugh, W. A., Null, S. E., & Kettenring, K. M. (2020). Restoring a saline lake to a range of water levels with noisy data and diverse objectives, .

Swenson, S., Chamber, D., & Wahr, J. (2007). Estimating geocenter variations from a combination of GRACE and ocean model output. *Journal of Geophysical Research*, *113*, B08410. doi:10.1029/2007JB005338.

Taylor, K. E. (2001). Summarizing multiple aspects of model performance in a single diagram. *Journal of Geophysical Research: Atmospheres*, *106*, 7183–7192. doi:10.1029/2000JD900719.

Tourian, M., Elmi, O., Chen, Q., Devaraju, B., Roohi, S., & Sneeuw, N. (2015). A spaceborne multisensor approach to monitor the desiccation of lake Urmia in Iran. *Remote Sensing of Environment*, *156*, 349–360. doi:10.1016/j.rse.2014.10.006.

ULRP (2015a). Foundation. URL: http://www.ulrp.ir/en/foundation/.

ULRP (2015b). Road-map. URL: http://www.ulrp.ir/en/road-map/.

UNEP, G. (2012). The drying of Iran's lake Urmia and its environmental consequences. *J. Environ. Dev*, *2*, 128–137.

Vicente-Serrano, S. M., Beguería, S., López-Moreno, J. I., García-Vera, M. A., & Stepanek, P. (2010). A complete daily precipitation database for north-east spain: reconstruction, quality control, and homogeneity. *International Journal of Climatology*, *30*, 1146–1163. doi:10.1002/joc.1850.

Vishwakarma, B. D., Devaraju, B., & Sneeuw, N. (2016). Minimizing the effects of filtering on catchment scale GRACE solutions. *Water Resources Research*, *52*, 5868–5890. doi:10.1002/2016WR018960.

Vishwakarma, B. D., Devaraju, B., & Sneeuw, N. (2018). What is the spatial resolution of GRACE satellite products for hydrology? *Remote Sensing*, *10*. URL: http://www.mdpi.com/2072-4292/10/6/852. doi:10.3390/rs10060852.

Vishwakarma, B. D., Horwath, M., Devaraju, B., Groh, A., & Sneeuw, N. (2017). A data-driven approach for repairing the hydrological catchment signal damage due to filtering of GRACE products. *Water Resources Research*, *53*, 9824–9844. doi:10.1002/2017WR021150.

Voss, K. A., Famiglietti, J. S., Lo, M., Linage, C., Rodell, M., & Swenson, S. C. (2013). Groundwater depletion in the middle east from GRACE with implications for transboundary water management in the Tigris-Euphrates-Western Iran region. *Water resources research*, *49*, 904–914. doi:10.1002/wrcr.20078.

Wurtsbaugh, W. A., Miller, C., Null, S. E., DeRose, R. J., Wilcock, P., Hahnenberger, M., Howe, F., & Moore, J. (2017). Decline of the world's saline lakes. *Nature Geoscience*, *10*, 816. doi:10.1038/ngeo3052.

Xie, P., Janowiak, J. E., Arkin, P. A., Adler, R., Gruber, A., Ferraro, R., Huffman, G. J., & Curtis, S. (2003). GPCP pentad precipitation analyses:

An experimental dataset based on gauge observations and satellite estimates. *Journal of Climate*, *16*, 2197–2214. doi:10.1175/2769.1.

Zarghami, M. (2011). Effective watershed management; case study of Urmia Lake, Iran. *Lake and Reservoir Management*, *27*, 87–94. doi:10.1080/07438141.2010.541327.

AppendixA.

We assessed the gridded precipitation datasets over the Urmia basin using the ground-based data. Among all datasets, we have selected those that had data after 2014 until 2019 (see table). Ground-based data for precipitation were not available after 2014. The in-situ data is collected through synoptic stations and rain-gauges of the Ministry of Energy, more than 257 rain-gauge daily time series in Iran throughout 1965–2013 (Figure 1). Before comparison, we controlled the quality and homogenized the precipitation time series according to Vicente-Serrano et al. (2010). We used a grid of a half degree over Urmia basin same as global gridded precipitation datasets. To reach a gridded data from in-situ at each month, we averaged the precipitation from stations at each grid. Finally, we obtained the monthly precipitation over the Urmia basin by aggregating gridded datasets and gridded in-situ.

we compared the in situ time series with the time series of the datasets (table AppendixA), using a Taylor diagram (Taylor, 2001), (cf. Figure A.13), which shows three types of statistics: the correlation coefficient, the Root Mean Square Difference (RMSD), and the standard deviation. Almost all global datasets show a fairly strong linear correlation with the ground-based data with a correlation coefficient of more than 0.75. Since metrics summarized the comparison in one value and does not give us the whole picture of errors. Therefore, we compared the Cumulative Distribution Function (CDF) of the over median folded error (OMFE) of all datasets over the period of 1983–2013 (see figure A.12). Finally, we selected the datasets with (OMFE) less than 5 % of the long-term average of the annual precipitation over the Lake Urmia basin (c.f. green box in figure A.12).

Table A.2: Summary of global precipitation datasets. Abbreviations in the data source(s) defined as: G, gauge; S, satellite; and R, reanalysis.

Dataset	Data source(s)	Resolution		Coverage		Reference
		Spatial	Temporal	Spatial	Temporal	
Gauge-Based Products						
PRECL	G	0.5° × 0.5°	1 mo	Global land	1948–2019	(Chen et al., 2002)
CPC	G	0.5° × 0.5°	1 d	Global land	1979–2019	
Satellite-Based Products						
GPCP	G, S	2.5° × 2.5°	1 mo	Global	1979–2019	(Adler et al., 2003)
CMAP	G, S	2.5° × 2.5°	1 mo	Global	1979–2019	(Xie et al., 2003)
PERSIANN-CDR	G, S	0.25° × 0.25°	3,6 h /1 d	60°S–60°N	1983–2019	(Ashouri et al., 2015)
CHIRPS	G, S, R	0.05° × 0.05°	1d	50°S–50°N	1981–2019	(Funk et al., 2015)
Reanalysis Products						
ERA5	R	0.25° × 0.25°	6 h/ 1 mo	Global	1979–present	(Hersbach, 2018)
NCEP 1	R	2.5° × 2.5°	6 h/1 d/ 1 mo	Global	1948–2019	(Kalnay et al., 1996)
NCEP 2	R	1.875° × 1.875°	6 h/1 d/ 1 mo	Global	1979–2019	(Kanamitsu et al., 2002)
MERRA-2	R	0.5° × 0.67°	1 d	Global	1979–2019	(Rienecker et al., 2011)

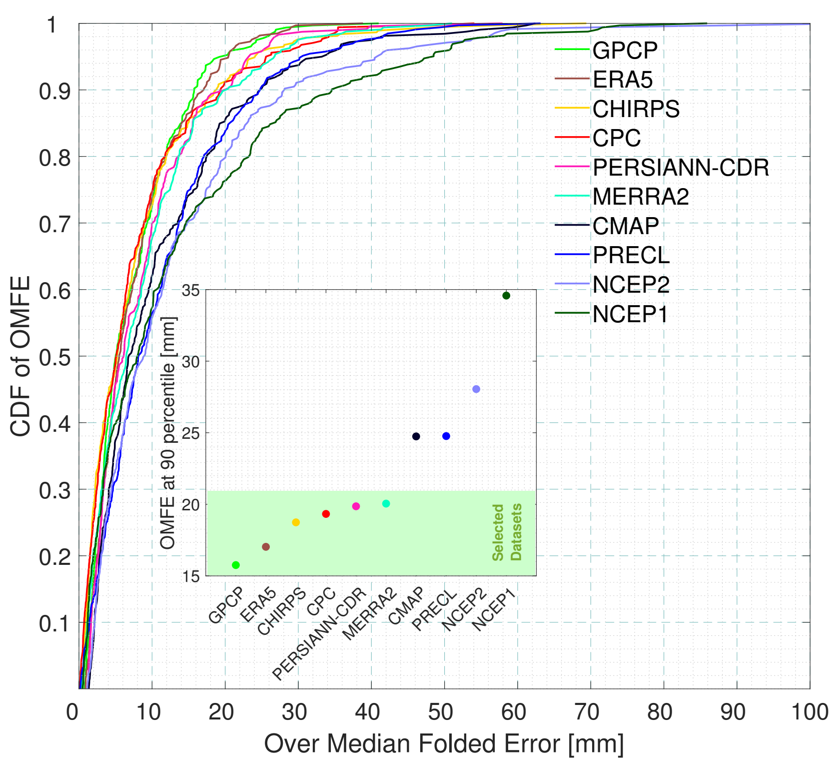

Figure A.12: cdf

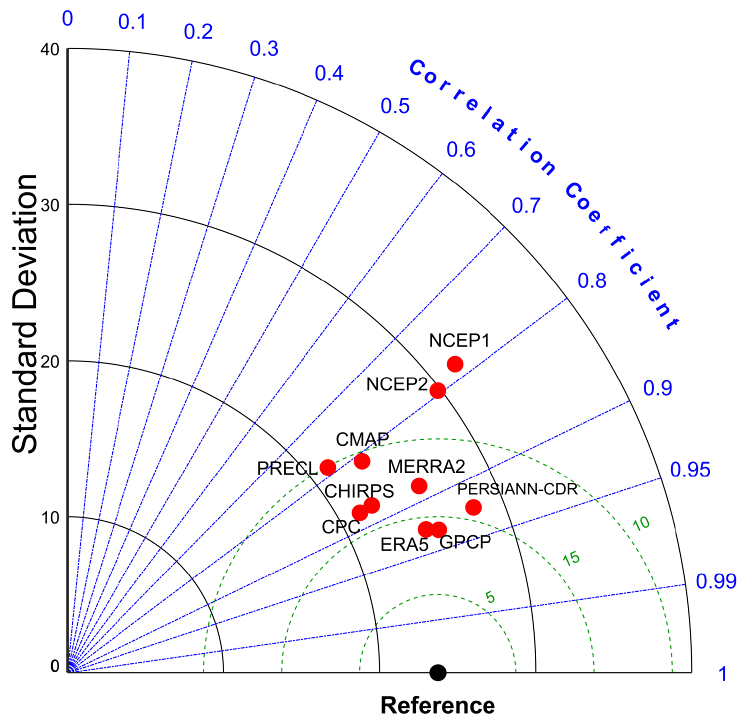

Figure A.13: Taylor diagram comparing global gridded precipitation datasets with in-situ precipitation data. Reference represents the in-situ data.

AppendixB.

To validate the ISODATA approach for extracting surface water extent over Lake Urmia, we compare our result with areas derived from the level-area curve in Figure B.14. The RMSE between the corresponding values of these two datasets is 488 km^2. Arabsahebi et al. (2019) extracted the time series of the lake's surface area using NDWI from Landsat 7 ETM+ satellite imagery. The accuracy of the ISODATA is slightly lower than the approach proposed by Arabsahebi et al. (2019). A better performance in the NDWI can be assumed due to the higher spatial resolution (30 m) compared to the coarse resolution of MODIS (250 m). It is important to mention that the bathymetry of the lake is not constant during the study period, mainly due to the sediment of salt to the bed of the lake. Therefore, for a better evaluation, a bathymetric map of the lake for some other period of 2002–2019 would be needed.

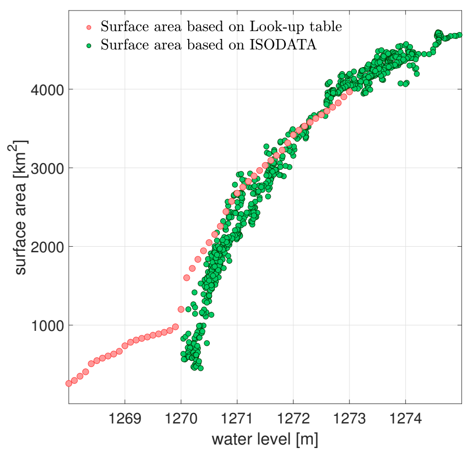

Figure B.14: Level-area curve based on ISODATA approach (grean dots) compared with the bathymetric map (red dots) for the time period from 2003 to 2017.